Iterative eigenvalue method using the Bloch wave operator formalism with Padé approximants and absorbing boundaries

Georges Jolicard,[1] David Viennot,[1] John P. Killingbeck,[1,2] and Jean-Marc Zucconi[1]
[1]*Laboratoire d'Astrophysique de l'Observatoire de Besançon (CNRS UMR 6091), 41 bis Avenue de l'Observatoire, Boîte Postale 1615, 25010 Besançon Cedex, France*
[2]*Mathematics Department, University of Hull, Hull HU6 7RX, United Kingdom*
(Received 2 March 2004; published 8 October 2004)

We present an iterative method for calculating eigenvalues and eigenvectors of large non-Hermitian matrices. The method uses an iterative procedure to solve the basic Bloch equation $H\Omega=\Omega H\Omega$ of wave operator theory. It involves nonlinear transformations such as the translation of diagonal matrix elements in the complex plane and the use of Padé approximants to treat the strongly coupled states which constitute an intermediate space around the model space. In the particular case of Floquet eigenstates the further step of adding time-dependent absorbing boundaries significantly improves the convergence properties of the iterative calculations.

DOI: 10.1103/PhysRevE.70.046703 PACS number(s): 02.70.Hm

I. INTRODUCTION

Studies of the rovibrational spectra of polyatomic molecules [1,2] and of the quantum dynamics of systems exhibiting resonances, as well as the Floquet analysis of photoreactive processes [3,4] are all faced with the task of calculating some internal eigenvectors of a large (possibly non-Hermitian) matrix [5]. In such applications the dimension N of the matrix is generally too large to use implementations of standard algorithms which store the full matrix and the cost of which in CPU time scales as N^3 [6].

These difficulties have prompted the development of iterative methods which do not store or modify the Hamiltonian matrix and which require only the computation of matrix-vector products. These methods can be classified into indirect and direct methods; the former include the relaxation method [7], the spectral method [8], and the filter diagonalization methods [9], while the latter include perturbative and moment method approaches. The most popular methods are variants of the algorithms of Davidson [10] or Lanczos [11–13] or of the filter diagonalization method.

A good method for calculating eigenvectors must (i) require the storing of only a small number of vectors (with dimension equal to that of the Hilbert space) and (ii) require the calculation of a reasonably small number of matrix-vector products to assure the convergence of the iterative process. From this viewpoint the Cullum and Willoughby (CW) Lanczos approach [14] and the filter diagonalization method [15–17], which extract energy levels from the same Krylov subspace, are operationally very similar and in both cases the CPU time mainly depends on the density of states. The CW Lanczos method [14] without regeneration of vectors easily satisfies (i) but in both methods many vectors must be stored or regenerated if eigenvectors are desired.

Hybrid techniques have been proposed in order to overcome some of the typical defects of the methods mentioned above; the Lanczos method has been coupled with a spectral filter [18] and a preconditioned Green function block algorithm has also been proposed [19]. A Lanczos algorithm which computes Lanczos vectors for $F(H)=(EI-H)^{-1}$ and which uses an inexact spectral transform to get exact energy levels has also been tested with success [20].

The calculation of resonance states and the use of a time-dependent Floquet formalism to investigate photoreactive processes leads to non-Hermitian matrices because of the use of complex absorbing potentials in the calculation of the matrix elements. The particular eigenvectors being sought will depend on the physical process being described. Photoreactive processes involve long-lived Floquet eigenstates with eigenvalues which have very small imaginary parts in the L^2 discrete representation as well as eigenstates which have a suitably large overlap with some specified initial state [21]. In such cases the diagonalization algorithm should be able to induce a state-to-state correspondence between the nonperturbed states (eigenvectors of H_0 or of $H_0-i\hbar\partial/\partial t$ for the Floquet dynamics in the extended Hilbert space [22]) and the perturbed states (eigenvectors of H_0+V or of $H_0+V-i\hbar\partial/\partial t$). The wave operator formalism has the capacity to follow continuously the eigenvectors as the perturbation develops as well as the advantage of selecting self-consistently the active space in which the greater part of the strong interaction is concentrated. This formalism satisfies criterion (i), since the number of stored vectors is equal to the dimension of the small active space and is constant during the iterations used in the recursive distorted-wave approximation (RDWA) algorithm [23] or in the single-cycle (SC) algorithm [24]. It has more difficulties in satisfying criterion (ii), particularly in the strong-coupling regime, but like the Lanczos method, has the advantage that it supports hybrid techniques; an approach which blends a Green function filter approach with wave operator techniques significantly improves the performances of wave operator iterative methods [25].

The present work presents an integration procedure for the nonlinear wave operator equation. The strategy adopted is to embed the active space in an intermediate space, within which nonlinear transformations such as complex translations of the diagonal elements or Padé transformations can be carried out to improve the convergence. In the case of Floquet eigenstates, a further procedure is used; the introduction of time-dependent complex boundary potentials gives a

natural spectral transformation which produces a notable improvement in the treatment of the Schrödinger equation in the Floquet picture.

The formalism is described in Sec. II, with an illustration involving the Floquet eigenstates of the ion H_2^+ interacting with a strong pulsed laser field. Particular attention is given to the Bloch wave operator formulation for the quasistationary treatment of the time-dependent Schrödinger equation. Section III sets out a time-dependent optical potential method which strongly modifies the Floquet spectrum and improves the convergence by selectively isolating the treated Floquet eigenstate. Section IV analyzes the results and gives some conclusions.

II. THEORY

A. Wave operator model in eigenvalue problems

The Bloch effective Hamiltonian theory was developed within nuclear physics and in quantum chemistry to improve on *ab initio* and semiempirical methods. The original wave operator concept was defined by Møller [26] within the context of scattering theory, while the later works of Bloch [27], Des Cloizeaux [28], and Durand [29] developed a theory more suitable for bound-state problems in nuclear physics and quantum chemistry.

The basic idea is to use the Hamiltonian H in the full Hilbert space to define an effective Hamiltonian H_{eff}, acting in a reduced model space S_0, such that a subset of the exact energy levels of H coincides with the energy levels of H_{eff}. Bloch sets the wave operator Ω equal to

$$\Omega = P(P_0 P P_0)^{-1}, \tag{1}$$

where P_0 is the projection operator of the model space S_0 and P is that of the corresponding active space S.

S is the subspace generated by the set of eigenvectors that play an important role in our problem. It can be constituted by eigenvectors which are situated in a given energy window or which possess a large overlap with a given unperturbed state. The model space S_0 is the space generated by the zero-order description of the states which constitute the active space S. If H is separated into $H=H_0+V$, then the elements of S_0 are usually eigenstates of H_0.

The wave operator Ω is the solution of a nonlinear equation

$$H\Omega = \Omega H \Omega \tag{2}$$

and leads to the effective Hamiltonian $H_{eff}=P_0 H \Omega$. By separating the wave operator into a diagonal and an off-diagonal part,

$$\Omega = P_0 + Q_0 \Omega P_0 = P_0 + X, \tag{3}$$

Eq. (2) can be written in the form

$$Q_0(1-X)H(1+X)P_0 = 0, \tag{4}$$

where 1 is the identity operator for the full Hilbert space and Q_0 the projector into the complementary space associated with the model space—i.e., $Q_0=1-P_0$.

Equation (4) manifestly displays the wave operator as a nonunitary and nonsingular transformation ($T=1+X$) which has a trivial inverse ($T^{-1}=1-X$) and which cancels the couplings between S_0 and S_0^+, generating H_{eff} from $P_0 H P_0$ by adding the term $P_0 H Q_0 \Omega P_0$.

The algorithm proposed in this paper integrates Eq. (4) and solves the eigenvalue problem inside S_0 by finding the reduced wave operator X, leading to Ω and thus to $H_{eff}=P_0 H \Omega$. The eigenvectors of H_{eff} are the projections into the model space of the corresponding exact eigenvectors. The wave operator transforms these projected eigenvectors back into the exact eigenvectors in the full space. Modern developments [21] show that the use of Eqs. (2) and (4) is not restricted to the treatment of stationary problems. The time-dependent Schrödinger equation can be transformed into an equation similar to Eq. (2) by working in an extended space. By introducing the time-dependent wave operator $\Omega(t)=U(t;H)[P_0 U(t;H) P_0]^{-1}$, the quantum evolution issuing from a model space S_0 can be factorized as follows:

$$U(t;H)P_0 = \Omega(t) U(t;H_{eff}). \tag{5}$$

Here the first evolution operator, associated with $H_{eff}(t)=P_0 H(t) \Omega(t)$, induces an evolution inside S_0 and the second term $\Omega(t)$ possesses an off-diagonal part which induces the transitions from S_0 into the complementary space S_0^+. The reduced wave operator is the solution of a nonlinear equation of motion:

$$i\hbar \frac{\partial X(t)}{\partial t} = Q_0[1-X(t)]H(t)[1+X(t)]. \tag{6}$$

If the perturbation is localized on a finite time interval $[0,T]$, Eq. (6) can be rewritten as

$$H_F(t)\Omega(t) = \Omega(t) H_F^{eff}(t) = \Omega(t) H_F(t) \Omega(t). \tag{7}$$

Equation (7) then resembles Eq. (2), provided that the Floquet Hamiltonian $H_F(t)=H(t)-i\hbar\partial/\partial t$ is taken in place of H. This implies that this modified eigenvalue equation should be solved in an extended Hilbert space

$$\mathbf{K} = \mathbf{H} \otimes \mathbf{L}^2(S^1, d\theta/2\pi), \tag{8}$$

where $\mathbf{H}$ is the initial Hilbert space and $\mathbf{L}^2$ denotes the space of square integrable functions on the circle of length 2π (with $\theta=2\pi t/T$). Within the formalism described above Eq. (2) now appears as a generic equation in the treatment of both stationary and dynamical problems. In the dynamical case it should nevertheless be noted that the Floquet eigenstates obtained by integration of Eq. (7) do not generally have the correct asymptotic behaviour, so that many Floquet eigenstates need to be combined to form an appropriate wave function. This aspect of the problem will be analyzed in Sec. III. In the next section the generic term H will be used to designate equally H or H_F.

B. Iterative integration of $H\Omega=\Omega H\Omega$

The task of integrating Eq. (2) or (7) has been handled using various iterative treatments [23,24]. Here we propose a variant of these methods and analyze more closely their convergence behavior; some aspects of the iterative techniques will be improved by using nonlinear transformations.

The important task is that of choosing the dimension N_0 of the model space S_0 and the mode of construction of S_0 around an initial unperturbed state $|i\rangle$. Various approaches to a suitable definition of S_0 have been proposed in the literature; these include the adiabatic reduced coupled equation method [30], the low-frequency expansion method [31], and several artificial intelligence techniques [32–34]. In our approach we use an algorithm based on the wave operator formalism. This procedure, called the wave operator sorting algorithm by Wyatt and Iung [2], is based on the iterative RDWA treatment of the Bloch equation [Eq. (2) or (7)]. After a finite number N_{max} of iterations a large number of states $|\alpha\rangle$ are connected by the RDWA iteration (generally less than 30 iterations are sufficient to connect all the space). The states $|\alpha\rangle$ are then reordered after state $|i\rangle$ such that those having the largest magnitudes of the reduced wave operator at an arbitrary iteration order $N \leqslant N_{max}$ are at the top end of the list. Nonconvergence of the iterations does not have serious consequence for this reordering. The model space S_0, the dimension N_0 of which is imposed in our model, is constructed by taking the N_0 first vectors. The ordering is also used to define an intermediate space of dimension N_1 adjoining the model space, simply by taking the N_1 next vectors. This intermediate space groups together the states which are strongly coupled to or are in near resonance with the states of the model space. It is this intermediate space which is subjected to nonlinear transformations in our treatment.

Starting from Eq. (2) or, equivalently, from Eq. (7), if $H \equiv H_F$ in an extended Hilbert space, a few algebraic manipulations lead to the equation

$$XH^{eff} - H'X = Q_0(H - H')X + Q_0HP_0, \tag{9}$$

with

$$H^{eff} = P_0H(P_0 + X).$$

This equation is true for any choice of the matrix H' in the complementary space $S_0^{\dagger}$; in the following H' will be assumed to be diagonal for simplicity.

By projecting Eq. (9) to the left on an arbitrary state $|f\rangle$ of the complementary space and by setting $E'_f = \langle f|H'|f\rangle$ one can arrive at an iterative integration procedure described by the equations

$$\langle f|X^{(n+1)} = \langle f|[Z + YX^{(n)}][P_0HP_0 + P_0HX^{(n)} - E'_fP_0]^{-1}, \tag{10}$$

with

$$Z = Q_0HP_0 \text{ and } Y = Q_0(H - H')Q_0.$$

Applying Eq. (10) requires inversion of the matrix $P_0(H + HX^{(n)})P_0 - E'_fP_0$ at each step of the iteration. The model space S_0 usually has a small dimension (typically $N_0 \leqslant 50$), so this inversion is without problems whenever the matrix H' is diagonal. One can then introduce the matrix $T^{(n)}$ which diagonalizes the effective Hamiltonian at the Nth step, so that

$$(T^{(n)})^{-1}[P_0H(P_0 + X^{(n)})]T^{(n)} = E^{(n)}_{eff}. \tag{11}$$

Equation (10) can then be transformed into the new iterative formula

$$\langle f|X^{(n+1)} = \langle f|[Q_0(H - H')X^{(n)} + Q_0HP_0] \times T^{(n)}[E^{(n)}_{eff} - E'_fP_0]^{-1}(T^{(n)})^{-1}. \tag{12}$$

The behavior of the sequence of iterates and more precisely the radius and speed of convergence of the iterative process directly depend on the choice of the arbitrary diagonal matrix H'. A simple choice is to identify H' with the diagonal part of H in $S_0^{\dagger}$. If one further assumes moreover that the model space is one dimensional with $P_0 = |i\rangle\langle i|$, one can transform Eq. (12) into

$$|i^n\rangle = \Omega^n|i\rangle = (1 + X^n)|i\rangle. \tag{13}$$

By setting $\Delta|i^{(n)}\rangle = (X^{n+1} - X^n)|i\rangle$ and $E^n_i = \langle i|E^{(n)}_{eff}|i\rangle$, one can finally write Eq. (12) as follows:

$$\Delta|i^{(n)}\rangle = (E^n_i - Q_0H_{diag}Q_0)^{-1}(H - E^n_i)|i^n\rangle. \tag{14}$$

This is exactly the iterative rule proposed in the Davidson algorithm [10].

A more sophisticated choice involves taking into account the effects of the couplings between S_0 and $S_0^{\dagger}$ on the diagonal matrix elements in the complementary space by setting

$$E'_f = (E'_f)^{(n)} = \langle f|(1 - X^{(n)})H(1 + X^{(n)})|f\rangle. \tag{15}$$

When introduced into Eq. (12) this choice leads to the RDWA approach proposed some years ago [23].

C. Nonlinear transformations

Although the iteration rule for the RDWA appears to be more sophisticated than that used in the method of Davidson, the performance of the RDWA-wave operator approach is sometimes poor compared to those of the Davidson and Lanczos methods. The reason is simple. Equation (12) is only used perturbatively in the wave operator approach; at step (n) the new wave operator is simply obtained by incrementation: $X^{(n+1)} = X^{(n)} + \Delta X^{(n)}$. By contrast the treatment is nonperturbative in both the Davidson and Lanczos approaches. At step (n) the Davidson treatment extracts energy levels from a Krylov subspace including $\{|i\rangle, \Delta|i^{(1)}\rangle, \Delta|i^{(2)}\rangle, \ldots, \Delta|i^{(n)}\rangle\}$ but requires the storing of a large number of vectors; this storage cost is too high to permit the treatment of Floquet eigenstates in large vector spaces. Our approach in this work is to improve the performance of the perturbative wave operator treatment by introducing artificial nonlinear transformations in order to take into account indirectly the strong-coupling effects introduced by the Krylov subspace.

Before explaining these transformations we should note that the wave operator formalism does incorporate in a nonperturbative manner some strong couplings—namely, those between the states which compose the model space; from a certain viewpoint the corresponding active space can be regarded as a Krylov space. However, the dimension of S_0 is necessary kept small to ensure the storage of only a small

number of vectors. Only the first few vectors which are strongly coupled and are in exact or near resonance are then selected in the model space. As all the states of the full space are ordered according to their importance in the eigenvector construction (see the wave operator sorting algorithm in Sec. II B), we can apply nonlinear transformations to the states of the intermediate space (states numbered from N_0+1 up to N_0+N_1+1), without explicitly constructing the corresponding eigenvectors. Two modifications of the iterative procedure are then proposed.

The first concerns the choice of the arbitrary diagonal matrix H'. The two previously mentioned choices led to iteration formulas like those of the Davidson theory and the RDWA treatment. However, the divergence of the wave operator iterations is more commonly caused by small denominators which are due to accidental near resonances between the eigenvalues of the effective Hamiltonian $H^{eff}=P_0(H+HX)P_0$ and the diagonal elements of $Q_0H'Q_0$. One way to suppress these effects is to identify $Q_0H'Q_0$ with the diagonal part of Q_0HQ_0, *except* for a reduced group of states, which are selected as the states of S_0^+ with eigenvalues nearest in the complex plane to the eigenvalues of the states included in the space S_0. These states belong to the intermediate space. For these states usually responsible for accidental resonances the corresponding diagonal elements H'_{jj} are chosen to be $H_{jj}+\delta_{jj}$, where the complex shift δ_{jj} is chosen to produce a suitably large minimum distance δE between H_{jj}^{eff} and the nearest eigenvalue of the complementary space S_0^+. In the simplest case of a one-dimensional model space, this option involves moving all the nearest eigenvalues outside a circle which is cenered on the effective eigenvalue and has the radius δE. This transformation is nonlinear, since it affects the denominator on the right-hand side of Eq. (12).

The second modification is the introduction of nonlinear transformations such as Padé approximants [35], Aitken's Δ^2 method [36], or the Borel transformation to improve the convergence. In our example, it is the diagonal $[N,N]$ Padé approximant which was used. The convergence criteria for Stieltjes series cannot be applied in the present case [37], but non-Stieltjes series have often been found to be summable using Padé methods [38]. The procedure which has been tested involves a two-step calculation. It is presented here in a simple form by assuming a one-dimensional model space but the generalization to degenerate model space is straightforward and is illustrated here by Fig. 2, below. During the first step the iterations using Eq. (12) are carried out up to a finite order N_{iter} (typically $N_{iter}\sim 20$). Simultaneously the N_1 states (j) of the intermediate space which generate accidental resonances are selected and the corresponding N_0N_1 series of N_{iter} elements are stored:

$$X_{j,i}^{n=0}, X_{j,i}^{n=1}, \ldots, X_{j,i}^{n=N_{\text{iter}}}, \quad j=1-N_p, \quad i=1-N_0. \tag{16}$$

The Padé procedure is applied to these series by considering successively the reals parts and imaginary parts using the scalar Wynn epsilon algorithm [35]. The transformation must be applied with caution; empirically the Padé approximant is found to be inefficient if the series considered is already well converged before applying the transformation. Consequently the convergence test

$$\sum_{n=N_{iter}}^{N_{iter}-3} |X_{j,i}^{n} - X_{j,i}^{n-1}| \leqslant \epsilon \tag{17}$$

was applied to each series (j,i) so as to exclude from the Padé procedure those which satisfied this criterion (typically $\epsilon=10^{-4}$).

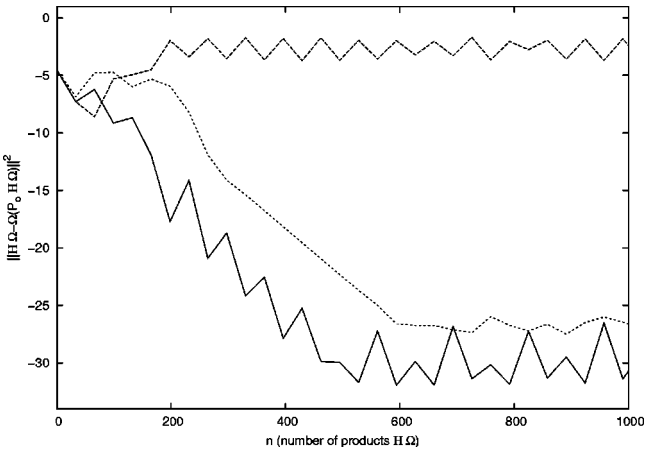

FIG. 1. Illustration of the effect of the choice of the matrix H' and of the use of the Padé procedure in the integration iterations using Eq. (12). The figure presents the defect $\|H\Omega-\Omega(P_0H\Omega)\|^2$ on a logarithmic scale as a function of the number of products $H\Omega$ formed during the computation. The three curves correspond to the three options: dashed line, $\delta E=0$, and no Padé procedure; dotted line, $\delta E=10^{-3}$ and no Padé procedure; solid line: $\delta E=0$, with the Padé procedure.

The Padé calculation leads to $N_P \leqslant N_0N_1$ complex values $(X_{j,i}^{\text{Padé}})$. In a second step, the iterations using Eq. (12) are continued, keeping these N_P components constant and equal to their Padé-extrapolated values. A test of convergence is made at the end of this second step. If the test is not satisfied, the two steps are repeated by starting with the nonconverged X operator.

The effects of these two nonlinear transformations are presented in Fig. 1. This figure shows, on a logarithmic scale, the quantity $\|H\Omega-\Omega(P_0H\Omega)\|^2$ for a one-dimensional model space as a function of the number of products HX formed during the computation.

The studied eigenvector is one generalized Floquet state of the H_2^+ molecule subjected to a Gaussian laser pulse which corresponds to an intensity of 4×10^{12} W/cm^2, with switch-on and -off times τ of 5 fs, and a plateau duration of $T_0=25$ fs, which is represented over a period T of 75 fs. The studied vector $\lambda_{v=0,n=0}$ corresponds to the unperturbed eigenstate $|v=0,n=0\rangle$—i.e., the ground vibrational state of the surface $^2\Sigma_g^+$ in the first Brillouin zone. The carrier wave frequency of the laser ($\omega_0=0.295\,868$ a.u.) is tuned in this case to the transition from $|v=0\rangle$ to the dissociative surface, so that the studied vector plays a central role in the photodissociation process [39]:

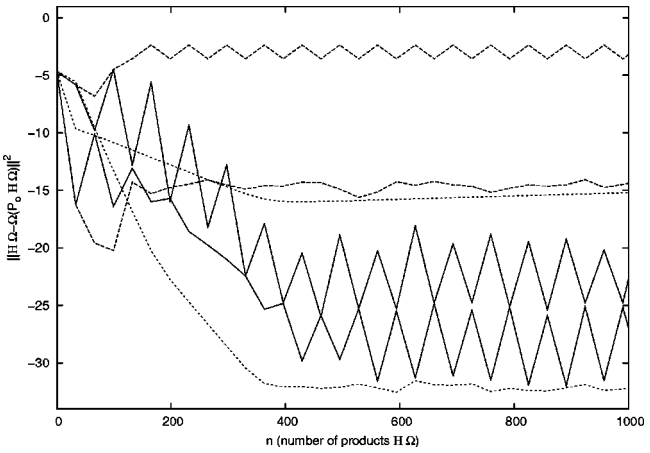

FIG. 2. The same as Fig. 1 but for the case of a two- dimensional model space. The pair of solid, dashed, and dotted lines correspond to the two Floquet eigenstates $\lambda_{v=0,n_1=0,n_2=0}$ and $\lambda_{v=1,n_1=-1,n_2=+2}$.

$$H_2^+\left(^2\Sigma_g^+, v=0, J=0\right)+\hbar\omega_0 \rightarrow H_2^+\left(^2\Sigma_u^+\right) \rightarrow H^+ + H(1s). \tag{18}$$

The complete basis introduces 102 400 states, from which $N_1=300$ are selected to constitute the intermediate space and eventually to participate in the Padé procedure. This figure reveals that the Padé procedure is highly effective in a case for which the standard wave operator series diverges strongly.

Figure 2 corresponds to a second caculation which involves two Gaussian pulses and a two-dimensional model space. The two intensities are equal to 2.25×10^{12} W/cm^2 and the two frequencies are tuned to the transitions: $\{^2\Sigma_g^+, |v=0\rangle\} \rightarrow \{^2\Sigma_u^+, E=E_{v=0}+\hbar\omega_1\} \rightarrow \{^2\Sigma_g^+, |v=1\rangle\}$. The model space includes the two dressed states $|v=0, n_1=0, n_2=0\rangle$ and $|v=1, n_1=-1, n_2=+1\rangle$ which are in exact resonance. The wave operator treatment makes it possible to collect into the model space all the states which are strongly coupled to the initial state or are in near resonance with it, as well as any other states which are of interest. This feature has a double advantage. First, all the eigenvalue-eigenvectors pairs are calculated at the same time. As a single wave operator Ω is stored during the calculation, the model space and the corresponding active space can include many vectors. Second, the strong couplings inside the model space are taken into account nonperturbatively by the effective Hamiltonian and the effects of these couplings on the exact eigenvectors are obtained by diagonalizing H_{eff}. In many circumstances this procedure reduces the number of iterations necessary to give a converged Ω giving a calculation which is faster than the separate calculation of the different exact eigenvectors included in the active space.

Figure 2 shows the improvements due to the two nonlinear transformations and particularly reveals the efficiency of the Padé procedure, which produces convergence of the two eigenvectors simultaneously up to a precision of 10^{-25}. For each pair of curves one column of the wave operator is observed to show better convergence than the other column. The difference is sometimes larger than 10^{10}. It is the column with the poorer convergence which imposes the precision of the final result, since the two columns are mixed together by the matrix which diagonalizes H_{eff} to form the Floquet eigenstates. In this framework the better results are obtained with the Padé approximants.

III. TIME-DEPENDENT ABSORBING BOUNDARIES

The filter diagonalization method significantly improves the performance of iterative methods for the eigenvalue problem. This method, which requires the calculation of products $(EI-H)^{-1}|i\rangle$, is computationally costly, even if the use of inexact spectral transforms appears as an interesting hybrid solution [20]. The Padé approximant procedure introduced in Sec. II is an alternative procedure which tries to obtain a good performance without needing a costly spectral transformation.

In the integration of Eq. (7), which represents the time-dependent Schrödinger equation (TDSE), one can use another spectral transformation method, called the "constrained adiabatic trajectory method" (CATM) [40]. This modifies both the spectrum and the Floquet eigenstates (unlike the standard filter diagonalization method) but it does not require the solution of a large linear system at each step. It is described below and is illustrated by treating again the Floquet states of the H_2^+ molecule subjected to a Gaussian laser pulse.

The approach exploits the equivalence which exists between the Schrödinger equation in the Hilbert space and the Floquet eigenequation in the extended Hilbert space and also the linear correspondence existing between the solutions—namely,

$$H_F(t)|\Psi(t)\rangle = 0 \Leftrightarrow (H_F - E)|\lambda\rangle = 0,$$

$$|\Psi(t)\rangle = \exp\left\{\frac{1}{i\hbar}Et\right\}|\lambda(t)\rangle. \tag{19}$$

Unfortunately this correspondence cannot be exploited in most cases because the eigenvalue E and also the initial value of the Floquet eigenstate $|\lambda(t=0)\rangle$ are imposed by the interaction. This initial value does not generally correspond to the initial value of the wave function [a usual choice identifies $|\Psi(t=0)\rangle$ with a nonperturbed molecular eigenstate $|i\rangle$]. The CATM solves this difficulty by artificially imposing the correct initial conditions. To do this the initial time interval $[0, T_0]$ over which the field-matter interaction takes place is prolonged by using an additional time interval $[T_0, T]$. Absorbing time-dependent potentials are then introduced along this extra time interval and on each molecular channel different from the initial one $|i\rangle$. These potentials are of the form

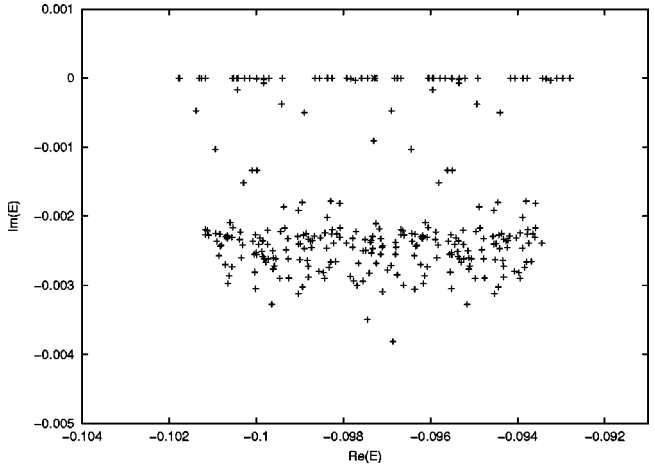

FIG. 3. The unperturbed Floquet spectrum of H_2^+ around the initial state without time-dependent absorbing boundaries. The star (∗) corresponds to the initial state $|i,n=0\rangle$.

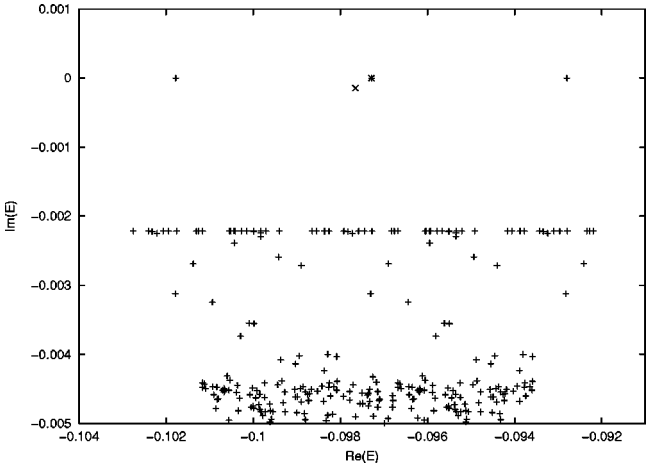

FIG. 4. The unperturbed Floquet spectrum of H_2^+ around the initial state when time-dependent absorbing boundaries are introduced asymptotically. The star (∗) corresponds to the initial unperturbed state $|i,n=0\rangle$ and the cross (×) to the corresponding Floquet state $\lambda_{i,n=0}$.

$$-iV_{opt}(t)=\sum_l |l\rangle\langle l|\left\{-iA\exp\left[-\left(\frac{t-\tau_0}{\tau}\right)^2\right]\right\}(1-\delta_{l,i}), \tag{20}$$

where τ_0 is equal to $(T_0+T)/2$ and τ is chosen such that V_{opt} is negligible at $t=T$.

The initial state corresponds here to the ground vibrational state $|v=0\rangle$ of the surface $^2\Sigma_g^+$ and to the first Brillouin zone: $|i,n=0\rangle$. The analyses developed in Ref. [40] reveal that two cases can be distinguished:

Case 1. Some Floquet eigenvalues are not affected by the introduction of the absorbing boundaries conditions. For such states the analysis proves that the absorbing boundaries impose negligible components $|\lambda(T)\rangle_{f\neq i}$ on the channels different from the initial one. As the Floquet eigenstates are periodic states by construction, this absorption imposes the initial expected conditions: $|\lambda(0)\rangle_k=\delta_{k,i}$ and finally [Eq. (19)] leads to an eigenstate proportional to the true wave function on the interval $[0,T_0]$. We note that because of the time arrow (from the past to the future) introduced by the TDSE the extra-time perturbation introduced after T_0 cannot retrospectively influence the true system before T_0.

Case 2. Other eigenvalues are greatly affected by the absorbing conditions and move about in the complex plane. In this case the eigenstates are disturbed in a chaotic way and cannot be used to solve the TDSE.

The basis is too large ($N=102\,400$) for us to calculate and present the exact spectrum of H_F. Nevertheless, partial analysis reveals that the distortion of the spectrum due to the field-matter interaction is small compared to that produced by the time-dependent boundary potentials. One can then roughly appreciate the influence of this spectral transformation by considering the unperturbed spectrum of $H_F^0=H_0-i\hbar\partial/\partial t$. Figure 3 presents the part of this spectrum around the eigenvalue of the initial state $|i,n=0\rangle$, without the presence of time-dependent absorbing boundaries.

The spectrum is complex because of the presence of two radial complex potentials placed asymptotically on the two potential energy surfaces for states $^2\Sigma_g^+$ and $^2\Sigma_u^+$. In Fig. 3 one can distinguish the bound states on the real axis and also a compact group of states which have an imaginary energy part larger than 2×10^{-3} a.u. in absolute value and which are related by a discretized representation of the continua of the two electronic states *g* and *u*. Some other intermediate states with a smaller imaginary energy part are present. They correspond to the highest bound states of *g* and their imaginary part is a pure numerical artifact without consequence for the dynamics. The spectrum is periodic with a period which corresponds to the time interval used—i.e., $[0,T]$. An important characteristic is that the initial state eigenvalue is embedded in a dense part of the spectrum on the real axis; this feature explains the difficulties in obtaining convergence of the numerical results in an iterative procedure.

Figure 4 represents the same spectrum after the introduction of time-dependent absorbing boundaries. It shows (near the real axis) the unperturbed eigenvalue $E_{i,n=0}(*)$ and the corresponding Floquet eigenvalue $E_{\lambda_{i,n=0}}(\times)$. Their positions reveal the small shift induced by the field-matter interaction. On the other hand, one notes a large translation of the spectrum in the lower half complex plane if one compares with Fig. 3 (the complex shift has an amplitude larger than 2×10^{-3}). Only the initial state and its duplications in the other Brillouin zones are not affected by this translation. The direct consequence is a beneficial dispersion of the eigenvalues around the initial one and a significant increasing of the distance between $E_{i,n=0}$ and the other nearest eigenvalues. This effect has important consequences for the iterative process using Eq. (12).

These consequences are confirmed by Figs. 5 and 6, which present the effect of the absorbing boundary procedure on the use of the iterative formula (12). In these two applications the laser field is intense ($I=1.6\times10^{13}$ W/cm^2 and $I=2.5\times10^{13}$ W/cm^2) and produces a rapid divergence of the

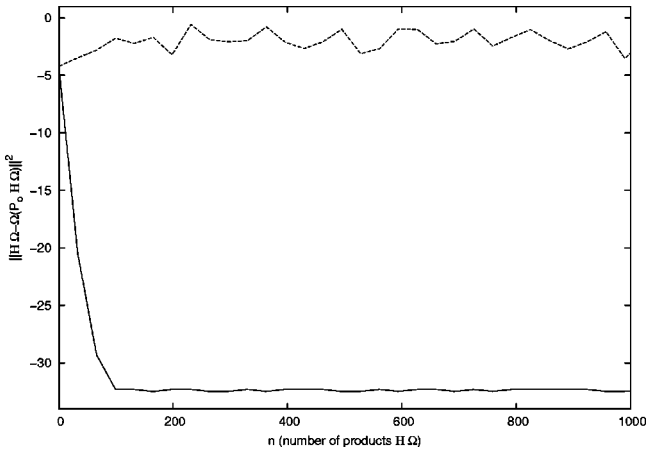

FIG. 5. Illustration of the effect of the time-dependent absorbing conditions in the integration of Eq. (12) for an intensity $I=1.6\times10^{13}$ W/cm^2. The figure presents the defect $\|H\Omega-\Omega(P_0H\Omega)\|^2$ on a logarithmic scale as a function of the number of products $H\Omega$ formed during the computation. The two curves correspond to the two options: dashed line, without absorbing boundaries; solid line, with absorbing boundaries.

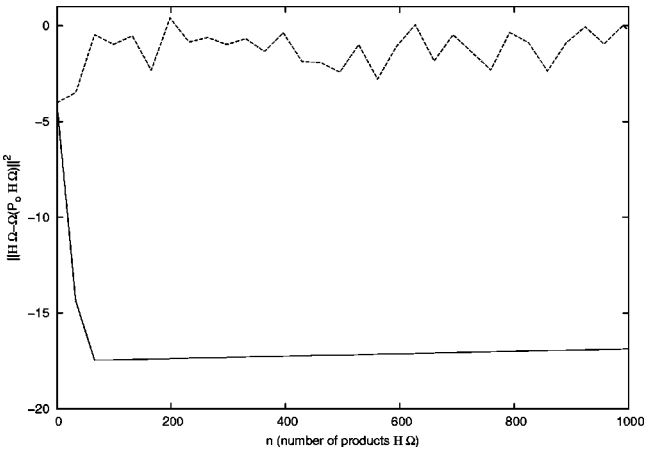

FIG. 6. The same as Fig. 5 but with an intensity equal to $I=2.5\times10^{13}$ W/cm^2.

iterative process. The introduction of complex boundary conditions drastically modifies this behavior and produces a convergence of the process after fewer than 100 iterations. The Floquet eigenvectors obtained by this procedure are also modified by the introduction of the boundary conditions but the proportionality between $|\Psi(t)\rangle$ and $|\lambda(t)\rangle$ represents a positive feature of this approach to the solution of the TDSE.

An important question concerns the performance of the present computational method as compared to those of other well-established methods: filter diagonalization and CW Lanczos methods. These three approaches are attractive for similar reasons: the large Hamiltonian matrix enters into the calculation only via the formation of matrix-vector products; moreover, only a few iterations are needed to converge widely separated eigenvalues. The loss of orthogonality in the Krylov spaces is a severe handicap for the single-vector Lanczos algorithm and the block Lanczos algorithm and requires selective [41] and partial reorthogonalization [42]. The Bloch treatment proposed here does not adopt a variational approach in a Krylov space. It identifies the states which make the solution process difficult and proposes a specific treatment of nonlinear transformations in the intermediate space which includes them. This reduces the nonorthogonality effects, even if reorthogonalizations are necessary in the precise calculation of resonance states in large spaces. For the same reasons the present treatment requires the storing of only a small number of vectors and finally makes possible the calculation of many eigenvalue-eigenvector pairs by calculating only once a multidimensional wave operator. The penalty is the less efficient behavior of our integration procedure in the strong-coupling regime. Figures 1 and 2 reveal that about 400 matrix products $H\Omega$ are necessary to converge the solution. Moreover, the two columns of the wave operator converge with notably different speeds in the degenerate case (Fig. 5), revealing that the Padé procedure has some difficulties in correlating the two vectors. Nevertheless, it should be recalled that the effects of large basis sizes and density of states are particularly severe for resonance calculations and that the efficiency of other approaches (such as for example the preconditioned inexact spectral transform [43]) depend critically on the effectiveness of the preconditioner used. In our case no preconditioner has been used.

The introduction of time-dependent absorbing potentials has strong positive effects (Figs. 5 and 6) and avoids the introduction of a spectral transform such as $F(H)=(EI-H)^{-1}$. However, this procedure is limited to the integration of the time-dependent Schrödinger equation and cannot be applied to solve stationary spectral problems.

IV. CONCLUSION

This paper treats the integration of the generic wave operator equation $H\Omega=\Omega H\Omega$, which describes stationary eigenproblems or quantum time-dependent dynamics according to the nature of the operator H and to the nature of the space in which it is defined.

The iterative solution method proposed is based on a standard RDWA procedure but is modified by using extra nonlinear transformations. Artificial translations of the diagonal matrix elements in the complex plane and Padé approximant transformations are tested; the second option appears as the better, especially when the active space on which the wave operator is defined is degenerate. The Padé approximant procedure forces the convergence of the iterative process by operating in a small intermediate space formed by states which are strongly coupled to the active space. The size of this intermediate space is small (200 or 300 in our examples) compared to the size of the full space ($>10^5$). The drastic improvement due to the nonlinear transformations consequently has a very small associated price in terms of increased CPU time requirements but the benefit in terms of improved convergence is important.

In the case of a nondegenerate Floquet eigenequation (i.e., if $H\rightarrow H_F$) we propose a spectral transformation based on the introduction of asymptotic absorbing boundary potentials

which control the asymptotic values of the periodic Floquet eigenstate and offer the possibility of forming a Floquet eigenstate proportional to the wave function which is a solution of the time-dependent Schrödinger equation. A second important effect of this transformation is to produce a translation in the complex plane of a great part of the spectrum. This spectral modification produces an increased distance between the Floquet eigenvalue investigated and the other nearest eigenvalues and so improves significantly the performance of the iterative process.

[1] D. Papousek and M.R. Aliev, *Molecular Vibrational-Rotational Spectra* (Elsevier, Amsterdam 1982).
[2] R.E. Wyatt and C. Iung, in *Dynamics of Molecules and Chemical Reactions* (Dekker, New York, 1996).
[3] J.H. Shirley, Phys. Rev. **138** B979 (1965).
[4] S.I. Chu, Adv. Chem. Phys. **73**, 739 (1989).
[5] N. Ben-Tal, N. Moiseyev, C. Leforestier, and R. Kosloff, J. Chem. Phys. **94**, 7311 (1991).
[6] W.H. Press, B.P. Flannery, S.A. Teukolsky, and W.T. Vetterling, *Numerical Recipes* (Cambridge University Press, Cambridge, England, 1989).
[7] R. Kosloff and H. Tal-Ezer, Chem. Phys. Lett. **127**, 223 (1986).
[8] M.D. Feit, J.A. Fleck, and A. Steiger, J. Comput. Phys. **47**, 412 (1982).
[9] D. Neuhauser, J. Chem. Phys. **93**, 2611 (1990); **95** 4927 (1991).
[10] E.R. Davidson, Comput. Phys. Commun. **53**, 49 (1989).
[11] C. Lanczos, J. Res. Natl. Bur. Stand. **45**, 255 (1950).
[12] G.H. Golub and C.F. Van Loan, *Matrix Computations* (Johns Hopkins University Press, Baltimore, 1989).
[13] R.G. Grimes, J.G. Lewis, and H.D. Simon, SIAM J. Matrix Anal. Appl. **15**, 228 (1994).
[14] J.K. Cullum and R.A. Willoughby, *Lanczos Algorithms for Large Symmetric Eigenvalue Computations* (Birkhäuser, Boston, 1985).
[15] M.R. Wall and D. Neuhauser, J. Chem. Phys. **102**, 8011 (1995).
[16] V.A. Mandelshtam and H.S. Taylor, J. Chem. Phys. **102**, 7390 (1995).
[17] V.A. Mandelshtam and H.S. Taylor, J. Chem. Phys. **106**, 5085 (1997).
[18] R.E. Wyatt, Phys. Rev. E **51**, 3643 (1995); J. Chem. Phys. **103**, 8433 (1995).
[19] T.J. Minehardt, J.D. Adcock, and R.E. Wyatt, Phys. Rev. E **56**, 4837 (1997).
[20] S.W. Huang and T. Carrington, J. Chem. Phys. **112**, 8765 (2000).
[21] G. Jolicard and J.P. Killingbeck, J. Phys. A **36**, R411 (2003).
[22] U. Peskin and N. Moiseyev, J. Chem. Phys. **99**, 4590 (1993).
[23] G. Jolicard and A. Grosjean, Phys. Rev. A **32**, 2051 (1985).
[24] J. Périé, G. Jolicard, and J.P. Killingbeck, J. Chem. Phys. **98**, 6344 (1993).
[25] G. Jolicard, J.P. Killingbeck, and M.Y. Perrin, Phys. Rev. E **63**, 026701 (2001).
[26] C. Møller, *Lectures on Elementary S-Matrix Theory* (NORDITA, Copenhagen, 1958).
[27] C. Bloch, Nucl. Phys. **6**, 329 (1958).
[28] J. Des Cloizeaux, Nucl. Phys. **20**, 231 (1960).
[29] Ph. Durand, Phys. Rev. A **28**, 3184 (1983).
[30] G.A. Voth and R.A. Marcus, J. Chem. Phys. **84**, 2254 (1986).
[31] W. Nadler and R.A. Marcus, J. Chem. Phys. **86**, 6982 (1987).
[32] J.V. Tietz and S.I. Chu, Chem. Phys. Lett. **101**, 446 (1983).
[33] J. Chang and R.E. Wyatt, J. Chem. Phys. **85**, 1826 (1986).
[34] C. Iung and C. Leforestier, J. Chem. Phys. **97**, 2481 (1992).
[35] J. Killingbeck, *Microcomputer Algorithms, Action from Algebra* (Adam Hilger, Bristol, 1991).
[36] C.M. Bender and T.T. Wu, Phys. Rev. **184**, 1231 (1969).
[37] G. Baker, Adv. Theor. Math. Phys. **1**, 1 (1965).
[38] E. Austin and J. Killingbeck, J. Phys. A **15** L443 (1982).
[39] G. Jolicard, O. Atabek, M.L. Dubernet-Tuckey, and N. Balakrishnan, J. Phys. B **36**, 2777 (2003).
[40] G. Jolicard, D. Viennot, and J.P. Killingbeck J. Phys. Chem. A (to be published).
[41] B.N. Parlett and D.S. Scott, Math. Comput. **33**, 217 (1979).
[42] H.D. Simon, Math. Comput. **42**, 115 (1984).
[43] B. Poirier and T. Carrington, J. Chem. Phys. **116**, 1215 (2002).